INSTITUTE OF PHYSICS PUBLISHING PHYSICS IN MEDICINE AND BIOLOGY

Phys. Med. Biol. **50** (2005) 1469–1482 doi:10.1088/0031-9155/50/7/010

Quantitation of the *a priori* dosimetric capabilities of spatial points in inverse planning and its significant implication in defining IMRT solution space*

Z Shou[1], Y Yang[1], C Cotrutz[1], D Levy[2] and Lei Xing[1]

[1] Department of Radiation Oncology, Stanford University, Stanford, CA 94305-5847, USA
[2] Department of Mathematics, Stanford University, Stanford, CA 94305-2125, USA

E-mail: lei@reyes.stanford.edu

Received 4 January 2005, in final form 2 February 2005
Published 16 March 2005
Online at stacks.iop.org/PMB/50/1469

Abstract

In inverse planning, the likelihood for the points in a target or sensitive structure to meet their dosimetric goals is generally heterogeneous and represents the *a priori* knowledge of the system once the patient and beam configuration are chosen. Because of this intrinsic heterogeneity, in some extreme cases, a region in a target may never meet the prescribed dose without seriously deteriorating the doses in other areas. Conversely, the prescription in a region may be easily met without violating the tolerance of any sensitive structure. In this work, we introduce the concept of dosimetric capability to quantify the *a priori* information and develop a strategy to integrate the data into the inverse planning process. An iterative algorithm is implemented to numerically compute the capability distribution on a case specific basis. A method of incorporating the capability data into inverse planning is developed by heuristically modulating the importance of the individual voxels according to the *a priori* capability distribution. The formalism is applied to a few specific examples to illustrate the technical details of the new inverse planning technique. Our study indicates that the dosimetric capability is a useful concept to better understand the complex inverse planning problem and an effective use of the information allows us to construct a clinically more meaningful objective function to improve IMRT dose optimization techniques.

(Some figures in this article are in colour only in the electronic version)

* Part of this work was presented in the 14th International Conference on the Use of Computers in Radiation Therapy, Seoul, Korea, 2004.

0031-9155/05/071469+14$30.00

1. Introduction

One of the implicit assumptions in current inverse planning is that all points within a target or sensitive structure are equivalent (Brahme *et al* 1982, Bortfeld *et al* 1990, Cho *et al* 1998, Gopal and Starkschall 2001, Holmes and Mackie 1994, Langer and Leong 1987, Spirou and Chui 1998, Webb 1991, Xing and Chen 1996, Zagars *et al* 2002). In reality, not all voxels have the same chance of complying with the prescription because the dose-limiting factors imposed by the involved sensitive structures are not uniformly distributed in space and the dose delivery is depth dependent. For a given patient and beam configuration, it is practically useful to know the likelihood for each individual point within a target or sensitive structure to meet its dosimetric goal. By understanding this intrinsic property of the system, one can better model the therapeutic plan optimization problem and improve the inverse planning techniques.

In this work, we introduce the concept of dosimetric capability for an arbitrary voxel in a target or sensitive structure to quantify the likelihood for the voxel to meet the specified dose. The capability calculation finds the potentially problematic regions and, more importantly, the degree of problems for these regions to meet their goals, and permits us to purposely modify the penalty strategy during the construction of objective function to minimize the problem. Mathematically, this process is realized by heuristically modulating the importance of the individual voxels according to the *a priori* capability distribution. The inverse planning formalism with dosimetric capability-modulated importance factors is applied to a few specific examples to illustrate the technical details. The approach sheds useful insight into the inverse planning problem and allows us to search for IMRT solutions that would otherwise be inaccessible.

2. Methods and materials

2.1. Definition of dosimetric capability

We quantify the likelihood for a voxel to meet its dosimetric goal by introducing the concept of dosimetric capability. Let us first consider the case of one incident beam. For a target voxel, the capability is assessed by the degree to which the voxel meets the prescription without violating the tolerance of the sensitive structure. The maximum achievable dose, $D^{\mathrm{ach}}(n_\sigma)$, at the voxel n_σ in the target is determined by scaling the intensity of the contributing beamlet to the highest value set by the tolerance of the sensitive structure. Mathematically, the 'capability', η, is defined as

$$\eta(n_\sigma) = \frac{D^{\mathrm{ach}}(n_\sigma)}{D_\sigma^{\mathrm{pre}}}. \tag{1}$$

The evaluation of equation (1) is straightforward for the case of a single incident beam or when there is no overlap of beamlets at the dose-limiting voxel in the sensitive structure. For multi-field IMRT, the $D^{\mathrm{ach}}(n_\sigma)$ is determined not only by those beamlets that directly intercept the voxel n, but also possibly by other beamlets irradiating different parts of the target. The coupled system can be described by a set of linear equations (which can be easily written from the above definition of the maximum achievable dose and the dose as a function of beamlet weights) and the $D^{\mathrm{ach}}(n_\sigma)$ of a target voxel will be obtained by optimizing the linear system, under the condition that the dose at any sensitive structure voxel is equal to its tolerance. The beam profiles so obtained deliver the maximum dose to the target without violating the tolerances of the sensitive structures. Mathematically, the system equations are underdetermined and a Cimmino algorithm (Stark and Yang 1988, Xiao *et al* 2000), which

was first applied to radiation therapy by Starkschal and Eifel (1992), can be used to find the solution. After assigning all beamlets with high enough initial intensities (say, two or three times the intensity values that deliver the prescribed dose to the target) and dose calculation, the calculation consists of the following steps.

(a) Choose a beamlet in a beam and locate the voxels in sensitive structures that are traversed by the beamlet.
(b) For each located voxel in the sensitive structures, check if the tolerance is exceeded. If yes, decrease the value of the beamlet based on

$$w_{jm}^{k+1} = w_{jm}^{k} + \lambda \sum_{n_\sigma} c_{n_\sigma}(w^k) d_{jm}(n_\sigma), \tag{2}$$

with

$$c_{n_\sigma}(w^k) = \begin{cases} \dfrac{\left(D_\sigma^{\mathrm{pre}} - D_c^k(n_\sigma)\right)}{\sum_{jm} d_{jm}^2(n_\sigma)} & \text{if } D_c^k(n_\sigma) > D_\sigma^{\mathrm{tol}} \text{ and } n_\sigma \in \text{sensitive structures} \\ 0 & \text{otherwise.} \end{cases}$$

(c) Update the dose.
(d) Repeat steps (b) and (c) until all voxels intercepted by the beamlet are checked.
(e) Repeat (a)–(d) for the next beamlet.

The above calculation is repeated until the doses in sensitive structures are equal to their tolerances. The relaxation parameter λ is generally set to a small value ($0.02 < \lambda < 0.1$) to ensure a smooth updating of the beamlet weights. The beamlet-by-beamlet updating scheme is similar to the simultaneous iterative inverse planning technique (SIITP) (Xing and Chen 1996). However, the goal here is to search for the beam profiles that deliver the highest achievable doses in the target, $D^{\mathrm{ach}}(n_\sigma)$, without violating the dose tolerance of the involved sensitive structures (in other words, any increase in the beamlet weights would lead to a dose exceeding the tolerance in one or multiple points inside a sensitive structure). Mathematically, the above calculation is an iterative projection algorithm converging to a feasible solution if the constraints are satisfied, otherwise to a compromise solution that minimizes the weighted sum of squares of deviations from the tolerance doses if dose constraints are violated.

The dosimetric capability of a voxel in a sensitive structure is characterized by the minimum achievable dose at the voxel needed in order to administer the prescribed dose to the target voxels. For consistency, we denote the minimum achievable dose by $D^{\mathrm{ach}}(n_\sigma)$ (where n_σ represents a voxel in the sensitive structure) and quantify the dosimetric capability of the voxel according to

$$\eta(n_\sigma) = \frac{D_\sigma^{\mathrm{tol}}}{D^{\mathrm{ach}}(n_\sigma)}. \tag{3}$$

For a voxel in a sensitive structure, the lower the minimum achievable dose, the more 'capable' the voxel is. The evaluation of equation (3) is once again straightforward for the case with a single incident beam. To obtain the minimum achievable dose, we first set the corresponding beamlet to such an intensity that the prescribed dose is delivered to the target voxels, and then evaluate the dose, $D^{\mathrm{ach}}(n_\sigma)$, at n_σ in the sensitive structure. For the case of multiple incident beams, a set of linear equations needs to be solved under the condition that the target voxels receive their prescription doses. Similar to the target case, the system equations become undetermined when there are multiple incident beams and a Cimmino algorithm is used to find the beam profiles that yield the lowest achievable dose in the sensitive structures. We first assign all beamlets with low enough initial intensities so that doses delivered to the target voxels are less than the prescription, and then do the following.

(a) Choose a beamlet in a beam and locate the voxels in the target that are traversed by the beamlet.

(b) For each located voxel in the target, check if the dose prescription is exceeded. If yes, lower the beamlet weight based on equation (2) with

$$c_{n_\sigma}(w^k) = \begin{cases} \dfrac{\left(D_\sigma^{\mathrm{pre}} - D_c^k(n_\sigma)\right)}{\sum_{jm} d_{jm}^2(n_\sigma)} & \text{if } D_c^k(n_\sigma) < D_\sigma^{\mathrm{pre}} \text{ and } n_\sigma \in \text{target} \\ 0 & \text{otherwise.} \end{cases}$$

(c) Update the doses.

(d) Repeat steps (b) and (d) until all voxels intercepted by the beamlet are checked.

(e) Repeat (a)–(d) for the next beamlet.

The above calculation proceeds iteratively until the target dose prescription is completely met for all voxels. We emphasize that the beam profiles obtained above are not intended to approximate the optimal fluence profiles for IMRT treatment. Instead, they are obtained purely for the purpose of evaluating the dosimetric capabilities of voxels in a target or a sensitive structure. Once the capability maps are obtained, they can be incorporated into an inverse planning procedure.

2.2. Incorporating dosimetric capability into inverse planning

The capability distribution contains information about the intrinsic heterogeneity of the dosimetric capability and reveals which points are likely to violate the prescription. The information provides a guiding map for the inverse planning algorithm to differentially deal with the regions having different chances of meeting their dosimetric goals. Our strategy is to assign a higher penalty (or high local importance) to those voxels with lower capabilities (those voxels are likely to have a dose lower than the prescription if they are in the target volume, or higher than the tolerance if they are located in a sensitive structure). While it is not difficult to intuitively conceive the general behaviour of the relation between local importance and the capability, the specific form of the relation is a matter of experimenting. The relation between the local importance and the capability used in our study is

$$\tilde{r}(n_\sigma) = (1 + g(n_\sigma)^2) r_\sigma, \tag{4}$$

where $g(n_\sigma)$ is empirically defined as

$$g(n_\sigma) = \begin{cases} \dfrac{3}{\left(\eta_\sigma^{\max} - 1\right)}(\eta(n_\sigma) - 1) & n_\sigma \in \text{target} \quad \text{and} \quad \eta(n_\sigma) \geqslant 1 \\ \dfrac{3}{\left(\eta_\sigma^{\min} - 1\right)}(\eta(n_\sigma) - 1) & n_\sigma \in \text{target or sensitive structure} \quad \text{and} \quad \eta(n_\sigma) < 1. \end{cases} \tag{5}$$

The capability map and the corresponding $\eta_\sigma^{\max}$ or $\eta_\sigma^{\min}$ are obtained for each structure. For a sensitive structure, if $\eta(n_\sigma) > 1$, it means that the voxel has no difficulty meeting its dosimetric goal and $g(n_\sigma)$ is set to zero. The differential penalty scheme allows the system to suppress potential hot spots in the sensitive structures and boost the potential cold spots in the target volume so that a more uniform dose distribution can be achieved in the target while sparing more sensitive structures.

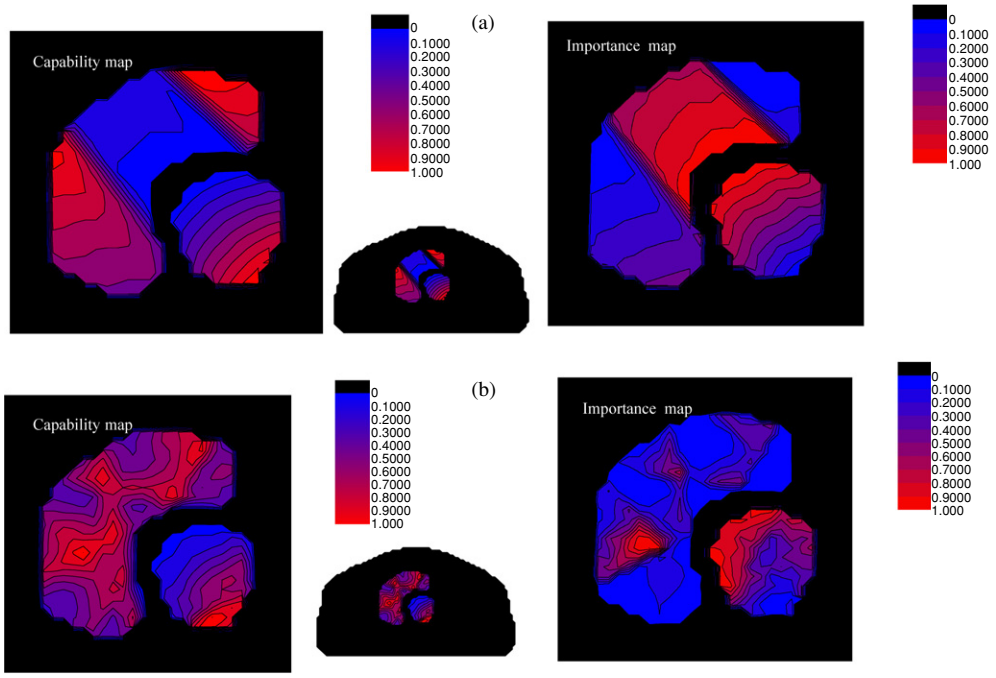

Figure 1. Dosimetric capability and importance maps of the target and sensitive structure for a hypothetical case for two beam configurations: (a) the single beam and (b) five equally spaced beams. The data for each structure are normalized to unity. For visual purposes, the capability and importance maps of the target and sensitive structure are enlarged and shown in the left and right panels for each beam configuration. The lower middle panel of each set of figures shows the complete geometry of the hypothetical structures.

2.3. Implementation

We implemented a software module to optimize the system in the platform of the PLUNC treatment planning system (an open source treatment planning system from the University of North Carolina, Chapel Hill, NC). The dose calculation engine and varieties of plan evaluation tools of the PLUNC system are used to evaluate and compare the optimization results. The SIITP (Xing and Chen 1996) was employed to obtain the optimal beam intensity profiles. The final IMRT plan is obtained in a similar manner to conventional inverse planning except that the uniform importance for the involved structures is replaced by the non-uniform importance distributions given by equations (4) and (5). The calculation was performed on a PC with P4 1.7 GHz and 1024 MB RAM.

2.4. Test of the new dose optimization formalism

To better understand the physics behind the capability calculation, we first constructed a hypothetical surrogate case (figure 1) and studied the behaviour of the system using a single beam and five incident beams. The gantry angle used for target irradiation in the single beam case was 320°, and in the five-beam case the angles used were 32°, 104°, 176°, 248° and 320°, where IEC convention for gantry angle is used. The incident photon energy was 15 MV. In both cases, the target was prescribed to 100 (arbitrary units) and the sensitive structure tolerance was set to be 25. An IMRT treatment was also planned with the same

Table 1. Summary of the parameters used for planning the IMRT prostate treatment. The tolerances of the sensitive structures are used in the evaluation of the capability maps.

	Prostate	Bladder	Rectum	Femoral heads	Skin
Importance factor	0.2	0.05	0.1	0.05	0.6
Prescription/tolerance	100	65	60	70	85

Table 2. Summary of the parameters used for planning the IMRT treatment of the paraspinal tumour. The tolerances of the involved sensitive structures are used in the evaluation of the capability maps.

	GTV	Spinal cord	Liver	Kidney	Tissue
Importance factor	0.86	0.03	0.005	0.05	0.055
Prescription/tolerance	100	30	40	30	75

five-beam configuration but structurally uniform importance factors, and the result was compared with the newly obtained plan. To ensure a fair plan comparison, in this and following examples the importance factors were chosen in such a way that the target DVHs were the same for the cases with uniform and non-uniform importance factors. The net improvements can then be assessed by the doses given to the sensitive structures.

The new algorithm was also applied to two clinical cases: a prostate case and a paraspinal tumour treatment. To illustrate the advantage of the technique, the results were compared with those obtained using the conventional inverse planning with uniform importance factors. For the prostate IMRT case, six equally spaced beams starting from 0° were used. Some relevant parameters used for planning the patient are summarized in table 1. As in conventional inverse planning, the structure-specific importance factors, $\{r_\sigma\}$, were determined by trial-and-error. To assess the new technique, we planned the case using three different strategies: (i) uniform importance for the prostate target and the sensitive structures; (ii) dosimetric capability-based non-uniform importance for the prostate target and uniform importance for all sensitive structures and (iii) dosimetric capability-based non-uniform importance for both prostate target and the sensitive structures. The three plans were compared using DVHs and isodose distribution plots.

In the paraspinal case, the sensitive structures involved include the spinal cord, liver and kidney. In this study, five 15 MV non-equally spaced coplanar beams (40°, 110°, 180°, 255° and 325°) were used for the treatment. The structure-specific importance factors and prescription/tolerances are summarized in table 2. IMRT plans with and without importance factor modulation were obtained and quantitative comparison was performed.

3. Results and discussions

3.1. A hypothetical test case

The capability and importance distributions for both single beam and five-beam configurations are plotted in figure 1. The isocapability and iso-importance curves are normalized to unity. For the single beam calculation (figure 1(a)), it is seen from the capability map (left panel) that the target region in the middle of the incident beam has lower dosimetric capability due to the restriction of the tolerance of the sensitive structure. For the points on both sides of the central target region, the dosimetric capabilities are much higher because of the absence

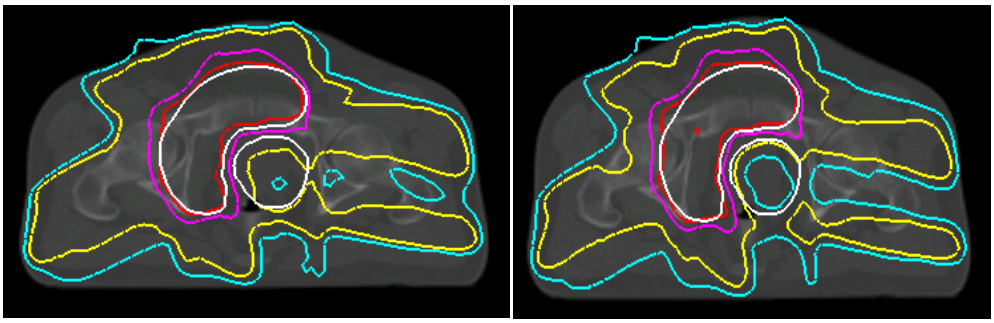

Figure 2. Isodose distributions for plans obtained without (left) and with (right) local importance factor modulation. The relative isodose curves labelled in the plots are, from the centre, 105% (red), 100% (pink), 80% (yellow) and 40% (blue), respectively.

of sensitive structure 'blocking'. The capability distribution within the sensitive structure can also be intuitively interpreted. For the voxels distant from the target volume, the capability is relatively high, indicating that these voxels are less dose-limiting points in comparison with the voxels close to the target. For the single beam case, the importance map (right panel of figure 1(a)) is almost an inversion of the capability map.

Figure 1(b) shows the capability and importance distributions when five incident beams are used to irradiate the target. The calculation is fairly efficient; it took less than 6 min for the system to obtain the capability and importance maps. In this case, the low capability region in the middle of the target shown in figure 1(a) disappears and only a few isolated low capability spots show up near the edge of the target. On the other hand, the overall behaviour of the capability map in the sensitive structure is not changed dramatically. The dosimetric capabilities for those points close to the target remain relatively low, which is consistent with our intuition since, relatively speaking, these points are more dose-limiting compared to the points far away from the target. The results also suggest that the boundary region between the two structures is likely to be underdosed (for target) or overdosed (for sensitive structure). In order to improve this, a non-uniform penalty scheme derived *a priori* or *a posteriori* becomes necessary. The technique described in this paper represents an example of the *a priori* method, whereas an adaptive adjustment of the local importance factor distribution would be an example of the latter. In general, the importance distribution is not a simple inversion of the capability map and depends also on the absolute values of the capabilities, as suggested by equations (4) and (5). This is especially true for the target, in which we need not only to 'boost' the potential cold region(s) but also to 'suppress' the potential hot spot(s). The high importance in the left-middle region of the target (see the right panel of figure 1(b)) is a direct consequence of the stated requirement. Indeed, a careful examination of the target capability data indicated that the region has high dosimetric capability and is thus likely to be overdosed. The assignment of higher local importance according to equation (4) permits us to suppress the potential overdosing *a priori*.

In figure 2, we show the IMRT plans obtained without and with modulating the spatial importance distribution. The left panel is the conventional IMRT plan with uniform importance factors assigned to both target and sensitive structures. The right panel shows the plan obtained with the spatially non-uniform importance distribution plotted in the right panel of figure 1(b). It is clearly seen that the isodose curves in the sensitive structure are 'pushed' towards the target and the dose gradient at the tumour boundary is greatly increased. The significant improvement can also be seen in the DVH plot (figure 3). It is remarkable that, by simply modulating the

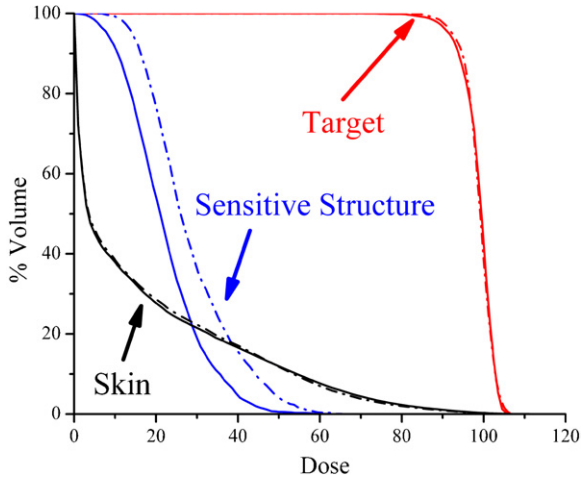

Figure 3. Target and sensitive structure DVHs corresponding to plans with two different penalty schemes: (a) uniform importance for every structure (dotted-dash curves) and (b) non-uniform importance for both target and sensitive structures (solid curves).

spatial importance distribution, an almost uniform reduction of ∼20% (normalized to the maximum sensitive structure dose) in the dose to the sensitive structure can be accomplished. If the dose to the non-sensitive structure normal tissue is not a limiting factor, the above result suggests that the target dose can be escalated by ∼10% while keeping the radiation toxicity at the current IMRT level.

3.2. Six-field IMRT prostate treatment

The IMRT plans obtained using three different penalty schemes are summarized in figures 4 and 5. The isodose distributions for the three penalty schemes are shown in figure 4. In figure 5, we compare the DVHs obtained using conventional inverse planning (dotted curves—obtained using uniform importance for the prostate target and the sensitive structures) and the new technique with non-uniform importance in both target and sensitive structures (solid curves). The DVHs of the plan with non-uniform importance to the prostate target and uniform importance to the sensitive structure are shown in dash-dotted curves. The importance factors for both target and sensitive structures were constructed based on the computed capability maps using the procedure described in section 2. It is seen from figure 4 that the dose sparing of the rectum and bladder is significantly improved when the non-uniform penalty scheme is employed. Remarkably, the maximum dose to the rectum is reduced from 68 to 60 and the fractional volume is dramatically reduced in the whole dose range. The reduction in the low dose region is more distinct, but the decrease in the high dose region is also evident and perhaps more clinically relevant. Similarly, significant improvements are achieved in the doses to bladder and femoral heads. For example, the fraction volume receiving a dose of 35 is decreased from 11% to 8% for bladder. The high dose tail in bladder is also evidently suppressed (from 70 to 66). Interestingly, the dose uniformity in the prostate target is also improved: the maximum dose of prostate target is slightly reduced from 110 to 107 and the minimum dose is increased from 85 to 87. In optimization, it is generally true that there is no net gain (that is, an improvement in the dose to a structure is often accompanied by dosimetrically adverse effect(s) at other points in the same or different structures). However,

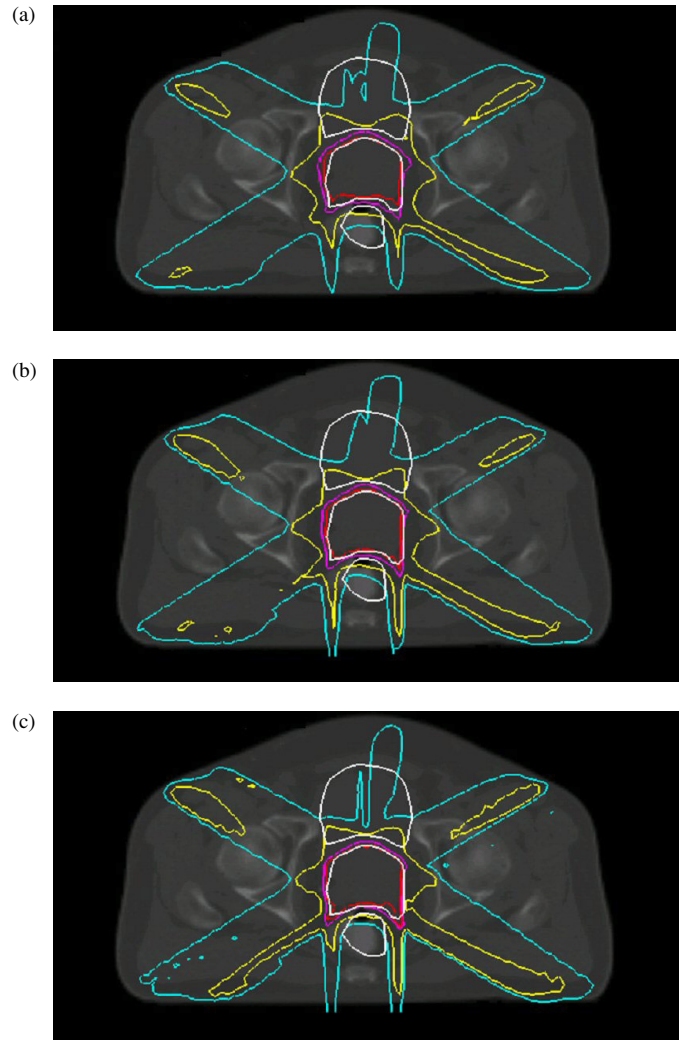

Figure 4. Isodose distributions obtained from three different penalty schemes: (a) uniform importance for every structure; (b) non-uniform importance for the prostate target and uniform importance for other structures and (c) non-uniform importance for every structure. From the centre, (red, pink, yellow and blue) curves represent 95%, 80%, 50% and 35% isodose curves. The 100% isodose curve corresponds to a dose of 72 Gy in this case.

one should note that things may be different when different penalty schemes are used, or more generally, when different objective functions are used. The simultaneous improvements in both target and sensitive structures here are a direct consequence of the enlarged solution space when non-uniform importance is permissible.

To better understand the technique, we have also optimized the dose under the condition that the non-uniform importance is allowed only for the prostate target (i.e., the importance for all sensitive structures is kept uniform). The corresponding isodose distribution is shown in figure 4(b) and the DVHs are plotted in figure 5 as dotted-dash curves. In this case, it is found that the target dose homogeneity is slightly improved. For example, the fraction receiving over 95 is increased from 91% to 96%. The maximum dose is reduced from 110 to 105.

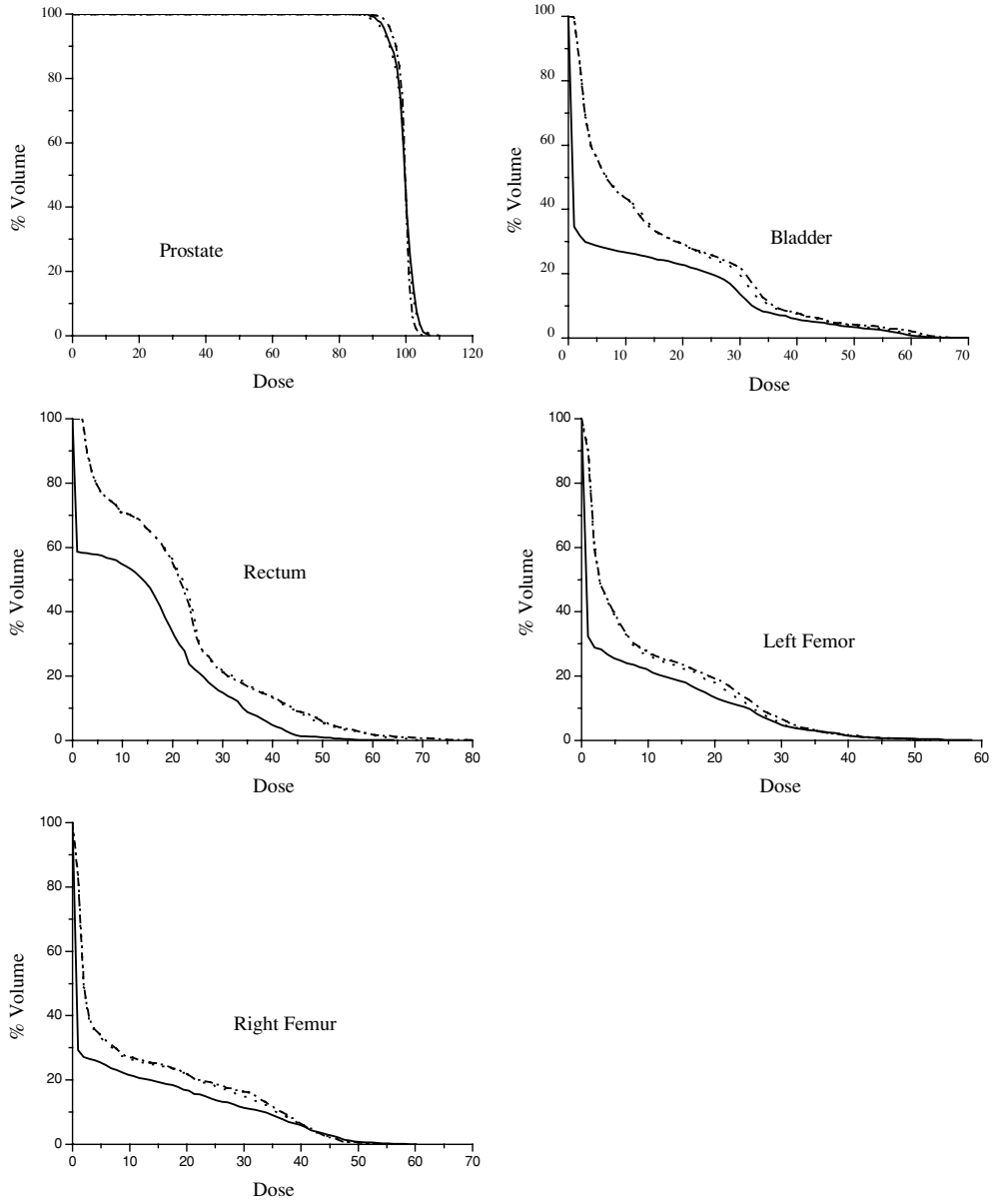

Figure 5. Target and sensitive structure DVHs corresponding to plans with three different penalty schemes: (a) uniform importance for every structure (dotted curves); (b) non-uniform importance for all structures (solid curves) and (c) non-uniform importance to the prostate and uniform importance to the sensitive structure (dash-dotted curves).

By individualizing the importance for the target voxels, we selectively increased the penalties to those voxels that are likely to be underdosed. Consequently, the target dose coverage is improved. It is interesting to note that there is essentially no change in the DVHs of the sensitive structures. The systematic improvement in the isodose distributions when the three different penalty schemes are employed can also be easily appreciated from figure 4.

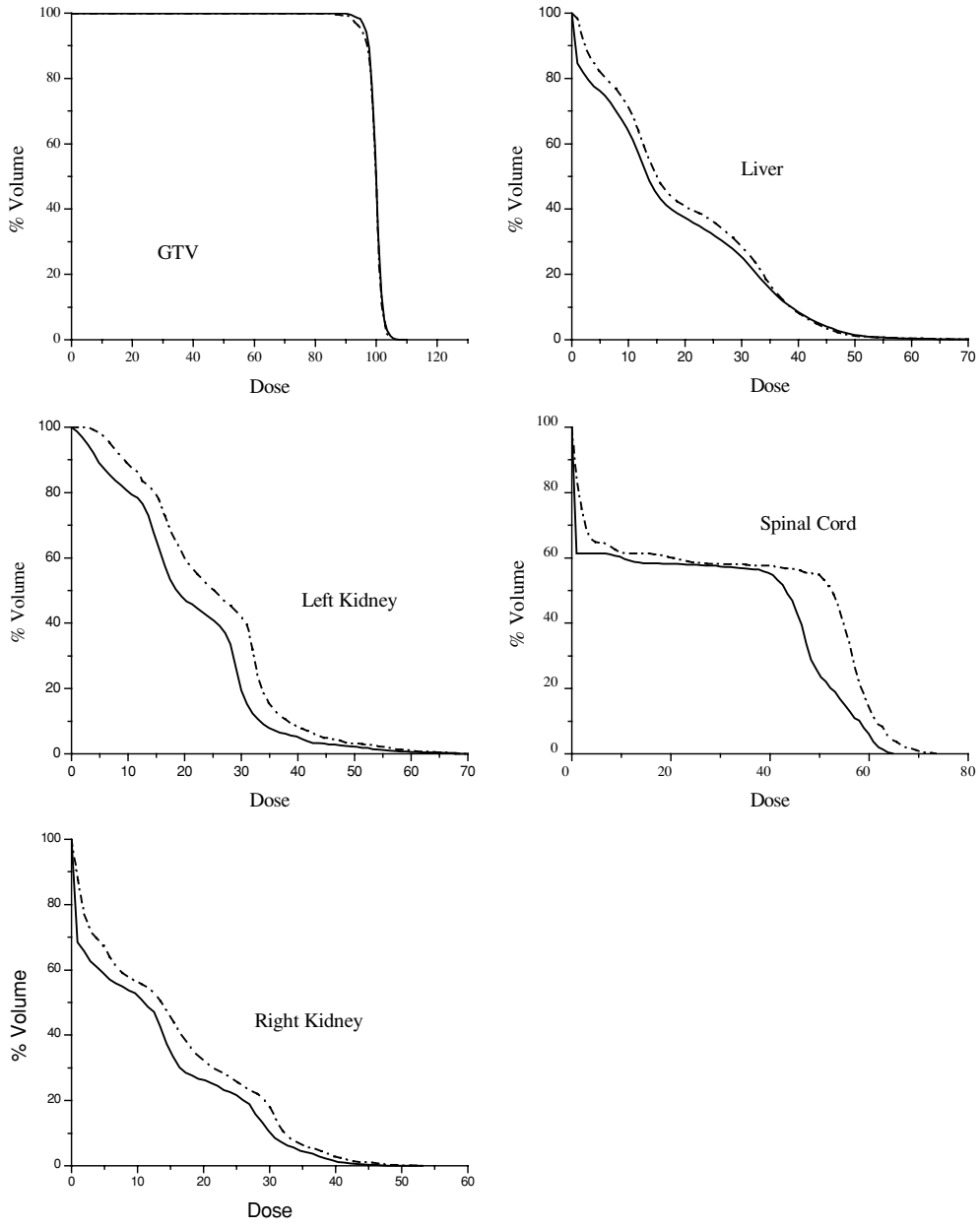

Figure 6. The comparison of DVHs for paraspinal tumour case between plan obtained from the algorithm proposed, denoted by solid line, and plan from conventional optimization, denoted by dotted dash line. The dose sparing of spinal cord, kidney and liver is evidently improved. The 100% in the x-axis corresponds to a dose of 56 Gy in this case.

3.3. Five-field IMRT treatment of a paraspinal tumour

The DVHs obtained using the conventional and newly proposed IMRT planning techniques are plotted in figure 6. The isodose distributions for the two plans are shown in figure 7. Similar

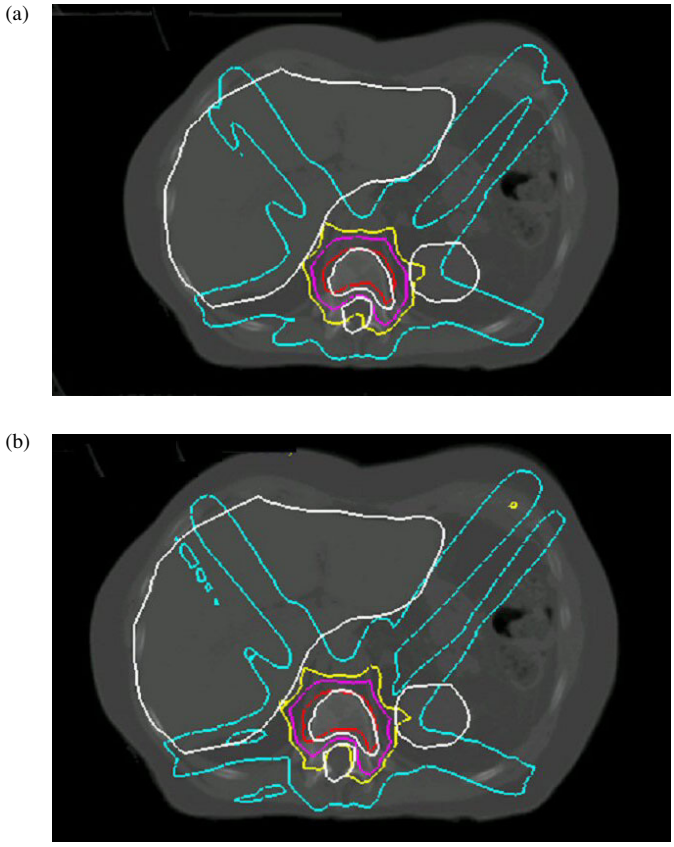

Figure 7. Isodose distributions for plans obtained with two different penalty schemes: (a) uniform importance for every structure and (b) non-uniform importance for every structure. From the centre, (red, pink, yellow and blue) curves represent 95%, 70%, 55% and 30% isodose curves.

to the previous case, when spatially non-uniform importance factors given by equation (4) are used, the target dose coverage and sensitive structure sparing are all improved in comparison with the conventional IMRT plan with uniform importance factors. For the target, the improvement is evident especially in the dose range from 90 to 95. The fractional volume receiving a dose level of 90 is slightly increased (from 99.3% to 99.7%). A more notable change is found for the fractional volume receiving doses higher than 95 (from 95.1% to 97.5%). The minimum target dose is increased from 84 to 90. The maximum target dose is, however, slightly increased from 105 to 106.5. By using the *a priori* non-uniform penalty scheme, it is found that the doses to the sensitive structures are dramatically improved. As seen from the DVHs, the spinal cord is better spared, especially in the high dose region. For example, the fractional volume receiving a dose above 50 dropped from 53% to 24%. The fractional volumes of the left kidney receiving a dose above 30 are reduced from 42% to 19% and for the right kidney, the reduction is about 7% (from 17.7% to 10.7%). The improvement for the liver is less impressive but evident. Once again, we would like to emphasize that the huge improvement in sensitive structure sparing is achieved without significantly deteriorating the dose coverage of the tumour target.

4. Conclusions

The dosimetric inequivalence of the voxels is a fundamental feature of the system and should be considered to obtain truly optimal IMRT plans. We have introduced the concept of dosimetric capability to quantify the likelihood for a voxel to meet its dosimetric goal and developed a new inverse planning formalism with the dosimetric capability-modulated voxel-dependent penalty. Using the new formalism, we can effectively 'boost' those regions where there are potential problems in meeting the dosimetric goals. With the aim of obtaining a spatially more uniform target dose distribution, in this paper, we presented a strategy to assign a higher penalty (or high local importance) to those voxels with lower capabilities. However, it is important to note that other penalty schemes can also be constructed under the guidance of the capability map to meet a different clinical requirement. The technique provides an effective mechanism to incorporate prior knowledge of the system into the dose optimization process and enables us to better model the intra-structural tradeoff. Comparison with the conventional inverse planning technique indicated that the algorithm is capable of generating much improved treatment plans with more conformal dose distributions that would otherwise be unattainable. Finally, we mention that the technique may find applications in dose optimization for many other radiation therapy modalities, such as prostate implantation, gamma knife, micro-MLC based stereotactic radiosurgery and other variants of IMRT, such as tomotherapy and intensity-modulated arc therapy.

Acknowledgments

We would like to thank Dr C Cameron for carefully reviewing the manuscript. The support of the Department of Defense (DAMD17-03-1-0657), the National Cancer Institute (5R01CA98523-02) and the Vadasz Family Foundation are gratefully acknowledged. The work of DL is supported in part by the NSF under Career Grant DMS-013351.

References

Bortfeld T, Burkelbach J, Boesecke R and Schlegel W 1990 Methods of image reconstruction from projections applied to conformation radiotherapy *Phys. Med. Biol.* **35** 1423–34

Brahme A, Roos J E and Lax I 1982 Solution of an integral equation encountered in rotation therapy *Phys. Med. Biol.* **27** 1221–9

Chen Y, Michalski D, Houser C and Galvin J M 2002 A deterministic iterative least-squares algorithm for beam weight optimization in conformal radiotherapy *Phys. Med. Biol.* **47** 1647–58

Cho P S, Lee S, Marks R J II, Oh S, Sutlief S G and Phillips M H 1998 Optimization of intensity modulated beams with volume constraints using two methods: cost function minimization and projections onto convex sets *Med. Phys.* **25** 435–43

Cotrutz C and Xing L 2002 Using voxel-dependent importance factors for interactive DVH-based dose optimization *Phys. Med. Biol.* **47** 1659–69

Cotrutz C and Xing L 2003 IMRT dose shaping using regionally variable penalty scheme *Med. Phys.* **30** 544–51

Das S, Cullip T, Tracton G, Chang S, Marks L, Anscher M, Rosenman J and Chang S X 2003 Beam orientation selection for intensity-modulated radiation therapy based on target equivalent uniform dose maximization *Int. J. Radiat. Oncol. Biol. Phys.* **55** 215–24

Gopal R and Starkschall G 2001 Plan space: representation of treatment plans in multidimensional space *Med. Phys.* **28** 1227

Holmes T and Mackie T R 1994 A comparison of three inverse treatment planning algorithms *Phys. Med. Biol.* **39** 91–106

Hristov D H and Fallone B G 1997 An active set algorithm for treatment planning optimization *Med. Phys.* **24** 1455–64

Langer M, Brown R, Urie M, Leong J, Stracher M and Shapiro J 1990 Large scale optimization of beam weights under dose–volume restrictions *Int. J. Radiat. Oncol. Biol. Phys.* **18** 887–93

Langer M and Leong J 1987 Optimization of beam weights under dose–volume restrictions *Int. J. Radiat. Oncol. Biol. Phys.* **13** 1255–60

Lian J and Xing L 2004 Incorporating model parameter uncertainty into inverse treatment planning *Med. Phys.* **31** 2711–20

Michalski D, Xiao Y, Censor Y and Galvin J 2004 The dose–volume constraint satisfaction problem for inverse treatment planning with field segments *Phys. Med. Biol.* **49** 601–16

Oelfke U and Bortfeld T 1999 Inverse planning for x-ray rotation therapy: a general solution of the inverse problem *Phys. Med. Biol.* **44** 1089–104

Olivera G H, Shepard D M, Reckwerdt P J, Ruchala K, Zachman J, Fitchard E E and Mackie T R 1998 Maximum likelihood as a common computational framework in tomotherapy *Phys. Med. Biol.* **43** 3277–94

Rosen I I, Lam K S, Lane R G, Langer M and Morrill S M 1995 Comparison of simulated annealing algorithms for conformal therapy treatment planning *Int. J. Radiat. Oncol. Biol. Phys.* **33** 1091–9

Spirou S V and Chui C S 1998 A gradient inverse planning algorithm with dose–volume constraints *Med. Phys.* **25** 321–33

Stark H and Yang Y 1988 *Vector Space Projections: A Numerical Approach to Signal and Image Processing, Neural Nets, and Optics* (New York: Wiley)

Starkschall G and Eifel P J 1992 An interactive beam-weight optimization tool for three-dimensional radiotherapy treatment planning *Med. Phys.* **19** 155–63

Thieke C, Bortfeld T, Niemierko A and Nill S 2003 From physical dose constraints to equivalent uniform dose constraints in inverse radiotherapy planning *Med. Phys.* **30** 2332–9

Webb S 1991 Optimization by simulated annealing of three-dimensional conformal treatment planning for radiation fields defined by a multileaf collimator *Phys. Med. Biol.* **36** 1201–26

Webb S, Convery D J and Evans P M 1998 Inverse planning with constraints to generate smoothed intensity-modulated beams *Phys. Med. Biol.* **43** 2785–94

Wu C, Olivera G H, Jeraj R, Keller H and Mackie T R 2003 Treatment plan modification using voxel-based weighting factors/dose prescription *Phys. Med. Biol.* **48** 2479–91

Wu Q, Mohan R, Niemierko A and Schmidt -Ullrich R 2002 Optimization of intensity-modulated radiotherapy plans based on the equivalent uniform dose *Int. J. Radiat. Oncol. Biol. Phys.* **52** 224–35

Wu X and Zhu Y 2001 An optimization method for importance factors and beam weights based on genetic algorithms for radiotherapy treatment planning *Phys. Med. Biol.* **46** 1085–99

Xiao Y, Galvin J, Hossain M and Valicenti R 2000 An optimized forward-planning technique for intensity modulated radiation therapy *Med. Phys.* **27** 2093–9

Xing L and Chen G T Y 1996 Iterative algorithms for inverse treatment planning *Phys. Med. Biol.* **41** 2107–23

Xing L, Li J G, Donaldson S, Le Q T and Boyer A L 1999 Optimization of importance factors in inverse planning *Phys. Med. Biol.* **44** 2525–36

Zagars G K, Starkschall G, Antolak J A, Lee J J, Huang E, von Eschenbach A C, Kuban D A and Rosen I 2002 Treatment planning using a dose–volume feasibility search algorithm *Int. J. Radiat. Oncol. Biol. Phys.* **53** 1097–105